HHS Public Access

Author manuscript

Prostaglandins Leukot Essent Fatty Acids. Author manuscript; available in PMC 2018 October 26.

Published in final edited form as:

Prostaglandins Leukot Essent Fatty Acids. 2018 September ; 136: 161–169. doi:10.1016/j.plefa.2017.01.002.

Lipidomic analysis reveals significant lipogenesis and accumulation of lipotoxic components in ob/ ob mouse organs

Jun Hayakawa[#a,2], **Miao Wang**[#a], **Chunyan Wang**[a], **Rowland H. Han**[a], **Zhen Y. Jiang**[b], and **Xianlin Han**[a,*]

[a]Center for Metabolic Origins of Disease, Sanford Burnham Prebys Medical Discovery Institute, Orlando, FL 32827, USA

[b]Department of Pharmacology & Experimental Therapeutics, Whitaker Cardiovascular Institute, Boston University School of Medicine, Boston, MA 02118, USA

[#] These authors contributed equally to this work.

Abstract

To further understand the role of lipogenesis and lipotoxicity in the development of obesity and diabetes, lipidomes of various organs from ob/ ob mice and their wild type controls were analyzed by shotgun lipidomics at 10, 12, and 16 weeks of age. We observed that the amounts of fatty acyl (FA) chains corresponding to those from de novo synthesis (e.g., 16:0, 16:1, and 18:1 FA) were substantially elevated in ob/ ob mice, consistent with increased expression of genes and proteins involved in biosynthesis. Polyunsaturated fatty acid species were moderately increased in the examined tissues of ob/ ob mice, since they can only be absorbed from diets or elongated from the ingested n-3 or n-6 FA. Different profiles of FA chains between ob/ ob mouse liver and skeletal muscle reflect diverging lipogenesis pathways in these organs. Amounts of vaccenic acids (i.e., 18:1(n-7) FA) in 12- and 16-week ob/ ob mouse liver were significantly increased compared to their controls, indicating enhanced de novo synthesis of this acid through 16:1(n-7) FA in the liver starting at 12 weeks of age. Coincidentally, synthesis of triacylglycerol from monoacylglycerol in the liver was also increased in ob/ ob mice starting at 12 weeks of age, as revealed by simulation of triacylglycerol synthesis. Moreover, levels of lipotoxic lipid classes were significantly higher in ob/ ob mice than their age-matched controls, supporting the notion that elevated lipotoxic components are tightly associated with insulin resistance in ob/ ob mice. Taken together, the current study revealed that lipogenesis and lipotoxicity in ob/ ob mice likely contribute to insulin resistance and provides great insights into the underlying mechanisms of diabetes and obesity.

Keywords

Lipidomics; Lipogenesis; Lipotoxicity; ob/ ob Mice; Obesity; Shotgun lipidomics

[*]Corresponding author. xhan@sbpdiscovery.org (X. Han).

[2]Current address: Biomarker R &D Department, Shionogi & Co. Ltd., Toyonaka, Osaka 561-0825, Japan.

1. Introduction

Prevalence of obesity and overweight is increasing at an alarming rate worldwide [1,2]. It is a critical public health concern in modern society associated with significant morbidity and mortality due to obesity-related complications, including insulin resistance, diabetes, cardiovascular, fatty liver diseases, inflammatory disorders, and certain cancers [3–9]. However, it is not yet fully understood how obesity leads to the development of these complications. Most believe that a combination of excessive food intake and lack of physical movement are primary drivers of obesity [10], but other potential causes include genetics, medical reasons, or psychiatric illnesses [11]. Some reports have also revealed other possible reasons for recently increasing obesity rates such as insufficient sleep [12], environmental pollution leading to fat accumulation [13], medications such as steroids which cause weight gain [14], and decreased variability of indoor ambient temperatures because of air-conditioners [15].

With the discovery of leptin which is produced predominantly in adipose tissue and regulates appetite by signaling on the central nervous system when food intake is adequate [16], the pathophysiology of obesity including regulation of appetite and food intake, storage patterns of adipose tissue, and development of insulin resistance has been further understood. Because storage of excess fat in peripheral tissues is a major factor contributing to obesity and type II diabetes, many investigators have related increased de novo lipogenesis and reduced fatty acid (FA) oxidation to adipose accretion in obesity, and are therefore studying the key lipid metabolizing enzymes [17–19] in order to primarily understand how obesity occurs and prevent its development. On the other side, extensive literature has stated that an increased adipose tissue mass leads to elevated nonesterified fatty acids (NEFA), which could mediate many adverse metabolic effects, including insulin resistance [17–19]. Especially, the overconsumption of n-6 polyunsaturated fatty acids (PUFA) and reduced intake of n-3 PUFA in daily diets, resulting in a high ratio of n-6 to n-3 PUFA, may also contribute to the increased pathogenesis of obesity by promoting chronic inflammation [20–22], since n-3 PUFA has shown anti-inflammatory effects in both healthy populations and in chronic inflammatory conditions, although more research is needed to fully evaluate the anti-inflammatory role of n-3 PUFA in the dietary management of obesity [23].

It has been reported that leptin significantly reduces hepatomegaly and liver triglyceride (TAG) levels by repression of the SCD-1 gene (stearoyl-CoA desaturase-1), which is the rate limiting enzyme for biosynthesis of monounsaturated fatty acids (MUFA) [24]. Therefore, leptin deficiency or leptin resistance in obesity leads to activation of SCD-1 and elevation of FA biosynthesis. It is known that increased synthesis and reduced oxidation of FA in adipose tissue lead to fat accumulation. Accumulation of certain lipids in non-adipose tissues could lead to cell dysfunction or cell death, and these processes have been generally described as lipotoxicity [25]. It is possible that excessive levels of “bad” lipid classes due to increased de novo lipogenesis or abnormal accretion of lipid metabolites contribute to lipotoxicity and development of insulin resistance, diabetes, and cardiovascular diseases [26,27]. Excessive lipid deposition and its pathogenic consequences have been well reported for liver, heart, pancreas, and muscle tissues [28–33]. However, temporal and spatial analyses of cellular

lipidomes in different tissues of ob/ ob mouse samples and lipotoxic deposition in these tissues have never been compared and reported systematically. Therefore, we believed that the accumulation of toxic lipid metabolites (such as NEFA, diacylglycerols (DAG), ceramide (Cer), or lysophospholipids) in muscle, liver, heart or other non-adipose tissues due to increased de novo lipogenesis could contribute to cell dysfunction or death, and develop into insulin resistance in obesity or other metabolic syndrome. In this study, in order to explore a potential link between lipid metabolites and obesity, cellular lipidomes from different organs of leptin deficient ob/ ob obese mice and their age-matched wild type controls were analyzed by multidimensional mass spectrometry-based shotgun lipidomics (MDMS-SL) [34–36]. We also measured the expression of a few genes which are relevant to de novo synthesis of long-chain fatty acids to confirm the increased lipogenesis in ob/ ob obese mice-.

2. Materials and methods

2.1. Materials

All synthetic phospholipids (di14:1 phosphatidylcholine (PC), di16:1 phosphatidylethanolamine (PE), di14:0 phosphatidic acid (PA), di 14:0 phosphatidylserine (PS) and di15:0 phosphatidylglycerol (PG)), lysophospholipid (17:0 LPC, 14:0 LPE) species, N-dodecanoyl sphingomyelin (N12:0 SM), and N-heptadecanoyl ceramide (N17:0 Cer) used as internal standards were purchased from Avanti Polar Lipids, Inc. (Alabaster, AL). Triheptadecanoylglycerol (T17:1 TAG) and 1,3-dipentadecanoin (1,3-D15:0 DAG) were purchased from Nu Chek, Inc. (Elysian, MN). Palmitic acid-d4 was obtained from Cambridge Isotope Laboratories, Inc. (Tewksbury, MA). All of the solvents were purchased from Burdick and Jackson (Honeywell International Inc., Muskegon, MI). All other chemical reagents of at least analytical grade or the best grade available were obtained from Sigma-Aldrich Chemical Co. (St. Louis, MO), Fisher Scientific (Pittsburgh, PA), or as indicated.

2.2. Animal model and tissue collection

Leptin-deficient ob/ ob (Lep^{-}/ Lep^{-}) mice and wild-type (Lep^{+}/ Lep^{+}) littermates (male) at 7 weeks of age were purchased from Jackson Laboratories (Bar Harbor, ME). Their genotypic information was provided by the vendor following the protocols of end point analysis, pyrosequencing, and restriction enzyme digest. Before being sacrificed, the mice were kept separately under a 23°C temperature and lighting-controlled house (12 h each of light and dark) with free access to a standard chow (Teklad Diet 2916, Harlan Laboratories, Indianapolis, IN) and water. Their body weights ranged from 22.2 to 27.3 g for WT and from 47.8 to 55.1 g for ob/ ob mice at 10 weeks of age, from 24.3 to 29.4 g for WT and from 51.7 to 59.1 g for ob/ ob mice at 12 weeks of age, and from 25.9 to 32.2 g for WT and from 55.8 to 64.7 g for ob/ ob mice at 16 weeks of age. At their age of 10, 12, and 16 weeks, respectively, eight mice (four WT and four ob/ ob in each age period) were euthanized by asphyxiation with carbon dioxide followed by cervical dislocation. Heart, liver, kidney, and thigh skeletal muscle tissue samples were excised quickly, perfused with ice-cold phosphate buffered saline (PBS) to remove blood, blotted with Kimwipes (Kimberly-Clark, Roswell, GA) to remove excess PBS buffer, and immediately freeze-clamped at the temperature of liquid nitrogen. All tissue samples were stored in a freezer at −80°C until lipid extraction

and analysis. Animal procedures were conducted in accordance with the “Guide for the Care and Use of Laboratory Animals” (National Research Council of National Academies, 2010) and approved by the Institutional Animal Studies Committee at the Sanford Burnham Prebys Medical Discovery Institute.

2.3. Preparation of lipid extracts and lipid derivatization

Mouse tissue wafers of interest were pulverized into a fine powder by a stainless steel Biopulverizer at the temperature of liquid nitrogen. Tissue fine powders (15–20 mg) were weighed from each sample and homogenized in 10× diluted PBS, and a protein assay on the homogenates was performed. All determined lipid levels were normalized to the protein content of individual samples. Lipid extraction from these mouse tissue homogenates was performed by a modified Bligh and Dyer method as previously described in details [37,38]. Generally, the bottom chloroform layers were collected; the solvents of the collected extracts were evaporated under nitrogen; and the residues after evaporation were resuspended in 200 μL of chloroform/ methanol (1:1, v/ v) per mg of protein for most of lipids analysis. All of the lipid extracts were flushed with nitrogen, capped, and stored at −20°C. Part of the lipid extracts (equal to 0.1 mg protein) were derivatized with N,N-dimethylglycine for analysis of DAG [39], and another part (equal to 0.05 mg protein) was reacted with N-[4-(aminomethyl)phenyl] pyridinium in order to measure the levels of NEFA, including their isomers as previously described [40,41].

2.4. Mass spectrometric analysis of lipids

MDMS-SL analyses were performed with a triple-quadrupole mass spectrometer (Thermo Fisher Scientific TSQ Vantage, San Jose, CA) equipped with an automated nanospray device (Triversa Nanomate, Advion Biosciences, Ithaca, NY) and operated with Xcalibur software as previously described [36,42]. Identification and quantification of all of the reported lipid molecular species, including NEFA, DAG, TAG, Cer, LPC, LPE, PC, PE, PS, PI, PA, SM [36,39,43] were performed using an in-house automated software program following the principles for quantification by MS as previously described in details with different MS/MS scans specific to each class of lipids [44,45]. FA chains of lipids were identified and quantified by neutral loss scans or precursor ion scans of corresponding acyl chains and calculated using the same in-house software program [36,39,44,46,47]. Quantification of individual lipid species was conducted in comparison to the selected internal standards of the classes. Tandem MS analyses of NEFA derivatives in the product ion mode for their isomer composition calculations were performed by using a Q-Exactive mass spectrometer (Thermo Fisher Scientific, San Jose, CA) equipped with an automated nanospray device under the same experiment parameters as described previously [40].

2.5. Gene expression by real-time RT-PCR

Total RNA was isolated from mouse skeletal muscle with an RNeasy fibrous tissue kit (Qiagen, Hilden, Germany) and real-time RT-PCR for the tissue samples was performed with an SYBR Green kit from Applied Biosystems by Life Technologies (Thermo Fisher Scientific, Carlsbad, CA) using specific primers. Target gene mRNA levels were normalized to cyclophilin using the ΔΔCt method and expressed as relative to the control.

2.6. Statistical analysis

All data were presented as the means ± SD of four separate animals for each group. Statistical significance was determined by a two-tailed Student t-test in comparisons with control, in which *$p < 0.05$, **$p < 0.01$, and ***$p < 0.001$.

3. Results

3.1. The levels of lipotoxic components markedly increased in ob/ ob mouse tissues

It has previously been reported that lipotoxicity plays a potential role in heart failure, obesity, and diabetes [48]. As anticipated, MDMSSL analysis of lipid extracts from the liver, heart, kidney, and skeletal muscle tissues of ob/ ob mice in comparison to their WT controls at 12 weeks of age revealed that the levels of lipotoxic lipid classes, including NEFA, DAG, TAG, Cer, LPC, and LPE, were significantly higher in the ob/ ob mice than their WT controls (Table 1). Additionally, NEFA levels in every examined tissue of ob/ ob mice were significantly higher than in that of their control counterparts. TAG levels were also higher in most ob/ ob mouse tissues. Levels of the majority of the lipotoxic lipid classes were significantly higher in the liver and heart of ob/ ob mice. Intriguingly, in contrast to the accumulation of lipotoxic components, MDMS-SL analysis showed that the levels of majority membrane lipids such as SM, PC, PE, and PS in ob/ ob mouse tissues were comparable to their WT controls (data not shown).

3.2. Lipotoxic components in ob/ ob mouse tissues accumulated in an age-dependent manner

A temporal comparison of the levels of lipotoxic components in the investigated tissue samples showed that the majority of them were increased in ob/ ob mice compared to their age-matched controls at 10, 12, and 16 weeks of age. Additionally, the ratios of levels in ob/ ob vs. WT controls were also different (Fig. 1). Most of the ratios of quantified lipotoxic lipid levels in the liver, muscle, and heart were higher at 16-week old than at 12-week old. For example, in the liver, the differences of total NEFA, DAG, TAG, Cer, LPC, and LPE levels between ob/ ob and WT mice were 2.8, 16.7, 56.7, 1.5, 1.7, 1.4-fold at 16 weeks of age versus 2.3, 4.6, 15.2, 1.8, 1.2, 1.4-fold at 12 weeks, respectively. In muscle and heart tissues, the ratios of some of the lipotoxic lipids were higher at 16 weeks compared to those at 12 weeks of age such as Cer and LPC, but others were not significantly different like LPE.

3.3. Ratios of fatty acyl chains in NEFA, DAG, and TAG pools of ob/ ob mouse liver and skeletal muscle relative to their WT control counterparts showed very different profiles

Dietary fatty acids are absorbed into the fatty walls of intestinal villi, some of which are reacylated again into TAG via DAG by diacylglycerol acyltransferase (DGAT) [49]. In order to understand the TAG synthesis process in different ob/ ob mouse tissues, we also investigated NEFA, DAG, and TAG FA chain profiles from liver and skeletal muscle of ob/ ob mice and their WT controls at 12 and 16 weeks of age. Ratios of these FA chains in ob/ ob mice compared to corresponding WT mice were calculated (Fig. 2). A significant increase of the majority of determined FA chains in the liver of ob/ ob mice vs. their controls was observed at 16 weeks of age, but the significant increases for the muscle tissues were

determined in 12-week-old mice. For the majority of the FA chains, the TAG pool showed the greatest increase in magnitudes (133.5 folds in the muscle and 142.7 folds in the liver), whereas the NEFA pool showed the smallest increases in both investigated organs.

3.4. Levels of de novo synthesized fatty acyl chains were significantly different in different lipid classes

FA chains are primarily biosynthesized in the liver and to a lesser extent in adipose tissue although a large proportion of FAs in mammalian are supplied from diet. De novo FA synthesis involves a few key enzymes: acetyl-CoA carboxylase (ACC), fatty acid synthase (FAS), SCD or FADS, and Elovl. Acetyl-CoA is carboxylated by ACC to form malonyl-CoA, and then the product is further converted into longer-chain FA like palmitic acid (16:0 FA) by FAS. Palmitic acids can be elongated to longer-chain FA with 18, 20, 22, or 24 carbon atoms by Elovl. Meanwhile, palmitic acid and other long-chain saturated FAs can be desaturated into the corresponding Δ7, Δ9, or Δ10 MUFA by SCD or FADS [50]. In this study, we investigated levels of FA constituents that come mainly from de novo synthesis, including FA 16:0, 18:1, and 18:0, in different lipid classes present in the liver and skeletal muscle of 16-week old ob/ ob mice and their controls (Fig. 3). The levels of 16:0, 18:1, and 18:0 FA chains were substantially elevated in most lipid classes in the liver of ob/ ob mice compared to WT. For example, 16:0 FA was increased in NEFA, TAG, DAG, and LPC with an increase of 81.4 folds in the TAG pool as an example; 18:0 FA was significantly elevated in every examined class, especially in the TAG pool in which an increase of 111.7 folds was demonstrated; and increases in 18:1 FA content were observed in all examined lipid classes except PE with the increase reaching 42.1 folds in the TAG pool in ob/ ob mouse liver relative to controls. However, in skeletal muscle of ob/ ob mice at 16 weeks of age, the levels of 16:0, 18:1, and 18:0 FAs were only elevated in the lipid classes of NEFA, DAG, and TAG compared to their WT controls. Moreover, increased magnitudes of lipids in the muscle were not as high as in the liver (Fig. 3).

Due to deficiency in Δ12 and Δ15 desaturases, mammalians cannot synthesize FA with double bonds beyond carbon 10, including α-linolenic acid (an n-3 FA) and linoleic acid (an n-6 FA). These FAs are required for maintaining normal functions of all body tissues, but cannot be synthesized de novo and must be ingested from diet [51]. Therefore, these families of FA (including both n-3 and n-6 FA) are called essential fatty acids. We also investigated the essential NEFA pools, including α-linolenic acids and linoleic acids, in the liver and skeletal muscle of 16-week old ob/ ob mice and their controls (Fig. 2). The results for the liver showed that levels of α-linolenic acids and linoleic acids were 0.90 ± 0.06 and 8.42 ± 0.68 nmol/ mg protein in ob/ ob mice compared to 0.59 ± 0.13 and 6.35 ± 0.95 nmol/ mg protein in controls, respectively. Levels of essential NEFA were increased only 1.3–1.5 times from control to ob/ ob mice. However, in the muscle, α-linolenic acids and linoleic acids were increased to 0.89 ± 0.15 and 9.89 ± 0.87 nmol/ mg protein in ob/ ob mice from 0.29 ± 0.04 and 3.93 ± 0.49 nmol/ mg protein in their controls, respectively, with an elevated ratio of 2.5–3.1 times.

Based on these results, we measured expression of a few genes which are relevant to de novo synthesis of long-chain fatty acids including fatty acid desaturase (FADS), stearoyl-CoA

desaturase (SCD), and very long chain FA elongase (Elovl) in skeletal muscles of ob/ ob and control mice at 16 weeks of age (Fig. 4). Significantly increased expression of the measured genes (FADS1, FADS7, SCD4, and Elovl7) in ob/ ob mice indicated that both FA elongation and desaturation were induced in skeletal muscle along with de novo lipogenesis of longer-chain FAs.

3.5. Levels of 18:1 NEFA isomers in liver, heart and skeletal muscle of ob/ ob mice varied relative to their control counterparts

Naturally-existing 18:1 NEFA includes three isomers, i.e., oleic acid (n-9), vaccenic acid (n-7), and petroselinic acid (n-12). In de novo synthesis of NEFA species, both palmitic acid (16:0 NEFA) and its metabolite produced by SCD-1 desaturation, 16:1(n-7) NEFA, can be further elongated by Elovl6 or Elovl5 to yield stearic acid (18:0 NEFA) and vaccenic acid, respectively. The resulting stearic acid can also be metabolized by SCD-1 to yield oleic acid [50], which is by far the most abundant MUFA in animal organs, both in structural lipids and deposited fats. Petroselinic acid is a main constituent of some plants, including carrots, parsley, and coriander [52], making it primarily dietary. In order to better understand which de novo synthesis pathway is activated in ob/ ob mice, we measured the percentage compositions of different 18:1 NEFA isomers in the liver, heart, and skeletal muscle of ob/ ob mice and their controls at 10, 12, and 16 weeks of age [40] (Fig. 5). At 12 and 16 weeks of age, the composition of vaccenic acid in the liver of ob/ ob mice was significantly increased, whereas oleic acid composition was decreased as compensation for the vaccenic acid. However, in other organs, like heart and skeletal muscle, the 18:1 FA isomer did not show apparent differences between ob/ ob and WT mice.

3.6. Bioinformatics simulation of TAG synthesis pathways

TAG species are mainly de novo synthesized through reacylation of DAG species by DGAT activities. The DAG species are mainly produced through dephosphorylation of PA, reacylation of MAG, and, to a much less degree, through hydrolysis of phospholipids such as PI. We recently successfully developed a dynamic simulation approach for understanding the remodeling processes of TAG based on these known biosynthesis pathways of TAG and MDMS-SL-derived data [46]. The parameters K1, K2, and K3, which are the probabilities of individual DAG pools being reacylated to TAG, were assigned to the contributions of the PA, MAG, and PI pathways, respectively. Therefore, the parameters derived from the simulation could be used to assess the relative contributions of different biosynthesis pathways to the TAG pool. From the lipidomics data of ob/ ob mice and their controls measured by MDMS-SL, we simulated the TAG biosynthesis pathways in the liver and muscle of mice at 10, 12 and 16 weeks of age (Fig. 6). In the liver, we found that the contribution of the PA pathway (i.e., K1) to the TAG pool decreased significantly in ob/ ob mice compared to their controls at 12 and 16 weeks of age (0.12 vs. 0.34 and 0.15 vs. 0.84, respectively). However, this pathway did not show significant changes between the ob/ ob and control mice at 10 weeks of age. It was further indicated that the other biosynthesis pathway of TAG, the MAG pathway (i.e., K2), in ob/ ob mice was markedly elevated at 12 and 16 weeks old. In the skeletal muscle, the K1 value (i.e., the PA pathway) ranged from 0.11 to 0.21, and it did not show any changes in the TAG biosynthesis pathways between ob/ ob mice and their controls at any age.

4. Discussion

4.1. The increases of lipotoxic lipids in ob/ ob mice were age and organ-dependent

These significantly elevated lipotoxic lipid levels in different ob/ ob mouse organs, including the liver, heart, muscle and kidney, comparing to their WT controls (Table 1) showed that excessive food intake led to the accumulation of NEFA in ob/ ob mice, which were subsequently converted into excessive TAG for storage. Alternatively, the high amounts of NEFA were converted into other lipid intermediates, raising levels of DAG, Cer, LPC, and LPE. These excessive lipid intermediate products could impair cellular function and cause lipotoxicity [30,53–55]. However, the levels of most membrane lipids were comparable in the investigated organs of the WT and ob/ ob mice (data not shown). These observations not only indicate that excessive amounts of lipotoxic intermediates, like LPC or LPE, originated from the excessive caloric intake rather than from degradation of membrane lipids, but also suggest that the accumulation of lipotoxic lipids is largely present in cytosol, in lipid droplets, or bounded to proteins. Thus, these intermediates might not impact much cellular membrane integrity, since it is widely accepted that lipid droplets are formed in the endoplasmic reticulum (ER) and bud from it [56]. Therefore, the cells in the organs were still functional although the contents of lipid droplets as cellular organelles were significantly elevated in this age period [57].

Lipidomic analysis of the ob/ ob mouse liver, muscle, and heart showed that the elevation of most quantified lipotoxic lipids comparing to WT counterparts was higher at 16-week old than 12-week old, and suggested that, in general, significantly elevated lipotoxic lipid levels at 16 weeks of age cause the inhibitory action on insulin signaling [58], since insulin levels and ratios of insulin vs. glucose in ob/ ob mice increase starting at around 13 or 14 weeks of age [59,60], indicating a transition from a normal insulin state to an insulin-resistant state. These findings are confirmed by the presently reported blood insulin-to-glucose ratios in ob/ ob mice, which were nearly 10 times higher in ob/ ob mice at 14 weeks than that at 11 weeks of age, and 45-fold greater than their WT controls [61]. It should also be emphasized that since ob/ ob mice at 12-week old are at the transition state of insulin resistance, it could be expected that many metabolic phenotypes are varied greatly during this state, which might explain the big variation occurred in the phenotype measurement as well as lipidomics results at this age (Table 1).

The lipidomics results indicating tissue-dependent increases in ratios of lipotoxic lipids at different ages suggested that either the accumulation of the lipotoxic lipids converted from excessive NEFA in non-adipose tissues, or the utilization of NEFA, or a combination of both were different in the investigated organs. Most of the accumulation, likely due to both de novo synthesis and storage, happened in liver tissues. Although the heart and skeletal muscle also showed a various degree of lipotoxic lipid accumulation, the accumulation of lipotoxic lipids in the kidney of ob/ ob mice was not apparent in comparison to their controls. It was reported that lipid-derived metabolites impair insulin signaling and activate inflammatory pathways, which leads to adipose tissue insulin resistance, release of excess NEFA into the circulation, and ectopic fat deposition in liver tissues [62]. Therefore, the liver behaves as the metabolic sensor of insulin resistance and a main target of lipotoxic status [63] and shows

the major accumulation of lipotoxic lipids. Excess NEFA content in plasma promotes skeletal muscle insulin resistance together with an increase of intramyocellular lipids [64], and the insulin resistance in skeletal muscle also more correlates with most lipotoxic lipid metabolites, such as Cer and/ or DAG [65,66]. Skeletal muscle is the target of circulating inflammatory cytokines, which causes its insulin resistance [67]. It has been reported that increased amounts of lipid deposits are detected in the myocardium of metabolic syndrome patients, and increased protein levels of SREBP-1c and PPARγ, suggesting activation of lipogenesis in those patients [68].

4.2. Elevation of lipogenesis in the skeletal muscle of ob/ ob mice

In the investigated tissues, the TAG pool mostly showed the greatest increases in ratios of ob/ ob comparing to WT mice (Figs. 2 and 3). This result is likely due to the storage of TAG de novo synthesized from NEFA and DAG. Levels of all excessively absorbed or synthesized NEFA and DAG were also significantly elevated in ob/ ob mice, but a large portion of these was reassembled into the TAG pool, which was differentially stored in the organs. Significant increases of TAG in the liver and skeletal muscle of ob/ ob mice at their different ages potentially indicate different TAG de novo synthesis pathways in these two organs as derived from dynamic simulation (see Subsection 3.6 and below). Alternatively, synthesized TAG was preferentially stored in the liver, but was also metabolized in the skeletal muscle to serve as fuel for muscular contraction. Whether this storage/mobilization process depends on insulin sensitivity or contributes to insulin resistance is unknown.

The measurement of biosynthesized FA constituents showed their different profiles and increased degrees between the liver and skeletal muscle (Fig. 3), which likely resulted from a combination of differential lipogenesis pathways and utilization in the liver compared to the skeletal muscle of ob/ ob mice. As to the essential NEFA, since they can only be ingested from food, the measurements of the FA profiles showed differences between the liver and skeletal muscle, which also reflect differential utilization of NEFA for further de novo biosynthesis and/ or energy deposition. As for other PUFA species, most were also elevated in a small degree in the investigated tissues of ob/ ob mice comparing to their controls, since they were mostly absorbed from diets or elongated from the ingested α-linolenic and linoleic acids (Fig. 2).

The gene expressions, including FADS, SCD, and Elovl, in skeletal muscle tissues confirmed that both FA elongation and desaturation were elevated together with de novo lipogenesis of longer-chain FAs. We believed that these pathways of lipogenesis in skeletal muscle contributed to the differences in their FA content composition compared to other ob/ ob mouse organs. It has also been reported that the SCD activity and levels of MUFA are increased in ob/ ob mouse heart tissues [59], indicating similarly induced lipogenesis pathways in ob/ ob mouse heart.

4.3. Composition of 18:1 NEFA in the liver for early diagnosis of diabetes

It has been reported that the composition of MUFA in the liver was pathophysiologically crucial in the process of obesity or metabolic syndrome [69,70]. Most MUFA are de novo synthesized through regulation of the genes FAS, SCD, FADS, and Elovl [71]. SCD-1

specifically was repressed by leptin and its RNA levels were highly elevated in ob/ ob mouse livers [72,73]. Mice lacking SCD-1 were resistant to obesity, as shown from the studies with SCD-$1^{-/-}$ knockout mice [24,74]. In our experiment, since the fed diets did not contain 16:1(n-7) NEFA or vaccenic acids, these increases of vaccenic acid composition in the liver of ob/ ob mice indicate that the de novo synthesis pathway from palmitic acid to 16:1(n-7) NEFA [40] by SCD-1 desaturation and subsequent production of vaccenic acid by Elovl5 was more activated in the liver of ob/ ob mice starting at 12 weeks of age. This activation occurred earlier than both signs of hyperglycemia and inhibitory actions on insulin signaling, which started around 13 weeks of age [60,75]. Therefore, it is possible that the composition of 18:1 NEFA in the liver could be used for early diagnosis of diabetes. Vaccenic acid produced from 16:1(n-7) NEFA by Elovl5 was previously shown to down-regulate gluconeogenesis in the liver [76]. The elevated vaccenic acid composition in the liver is likely a mechanism of self-protection for ob/ ob mice to decrease glucose production in response to fat accumulation and possible hyperglycemia.

A similar composition of different 18:1 NEFA isomers present in the skeletal muscle and heart of ob/ ob mice compared to WT indicate potentially different lipogenesis pathways in these tissues compared to the liver. Moreover, the data suggest that the de novo biosynthesis pathways from palmitic acid to both vaccenic acid and oleic acid were activated equally in the muscle and heart. Therefore, the levels of total 18:1 NEFA elevated in the ob/ ob mouse tissues without the changes of isomer composition.

4.4. Altered TAG biosynthesis in the liver and skeletal muscle

Excess energy intake largely stored in adipose tissues as well as other peripheral organs, has been frequently considered a causal factor of pathophysiological complications associated with metabolic syn drome [77], and the main biological role of TAG species is to serve as an energy storage depot. Therefore, it is important to elucidate the TAG biosynthesis pathways leading to differential accumulation of TAG in the organs of ob/ ob mice relative to WT controls.

The simulation of the TAG biosynthesis pathways through our lipidomics data of liver tissues in ob/ ob mice and their controls (Fig. 6) indicate that the PA pathway decreased and the MAG pathway was markedly elevated at 12 and 16 weeks of age, consistent with previous observations [78] that the deposition of excess energy into the TAG pool dominated in mouse liver due to excessive digestion and uptake of FAs in ob/ ob mice.

Significant increases of the PA pathway in the liver of 16-week old control mice compared to 12-week old mice (Fig. 6) was also consistent with the decrease of TAG levels from 62.13 nmol/ mg protein (Table 1) at 12 weeks old to 20.67 nmol/ mg protein at 16 weeks of age. The TAG deposition from food intake was decreased at 16 weeks old in control mice. Therefore, an important reason leading to obesity could be that much more intake energy was deposited in the liver through the MAG biosynthesis pathway in ob/ ob mice, although most of excessive energy was stored in the adipose tissue as the form of TAG.

In skeletal muscle, the TAG biosynthesis pathways did not show any changes between ob/ ob mice and their controls at any age. However, it still demonstrated that, even at a less

degrees, de novo synthesis of TAG through the PA pathway existed in skeletal muscles tissues.

5. Conclusions

In the current work, cellular lipidomes of the heart, liver, kidney, and skeletal muscle were measured in ob/ ob mice relative to their WT controls at 10, 12, and 16 weeks of age by MDMS-SL. The levels of lipotoxic lipid classes, including NEFA, lysophospholipids, Cer, DAG, and TAG in ob/ ob mice were significantly higher than in the controls, but the ratios of these lipids were different in an age and organ-dependent fashion. The amounts of FA chains (i.e., 16:0, 18:0, and 18:1 FA) representing de novo synthesis of fatty acids were substantially elevated in ob/ ob mice, consistent with increased expression of FA elongase and desaturase genes in the muscle. Different profiles of FA chains indicate that lipogenesis pathways in ob/ ob mouse liver and skeletal muscle are different, in addition to differential utilization of the biosynthesized lipids. It is the first time to find a significant elevation of lipogenesis in the skeletal muscle of ob/ ob mice. Most of PUFA species were moderately elevated in the investigated tissues of ob/ ob mice, since n-3 and n-6 FA cannot be biosynthesized by mammalians and were mostly absorbed from diets or elongated from the ingested α-linolenic and linoleic acids. Measurement of NEFA isomers showed that the composition of vaccenic acids in the liver of ob/ ob mice at 12 and 16 weeks of age was significantly increased compared to their lean controls, indicating that the de novo synthesis pathway from palmitic acid to 16:1(n-7) NEFA and then to vaccenic acid was more activated in the liver starting at 12 weeks of age. Coincidentally, the MAG to TAG biosynthesis pathway in the liver was also more activated in ob/ ob mice starting at 12 weeks of age as determined by TAG synthesis simulation. These results are consistent with increased deposition of excess energy in mouse liver due to excessive intake of food in ob/ ob mice. Collectively, through the temporal and spatial analyses of cellular lipidomes of peripheral organs, the tight association of de novo lipogenesis and lipotoxicity with insulin resistance in these investigated ob/ ob mouse organs provides great insights into the possible mechanism(s) underlying obesity, diabetes and related complications.

Acknowledgements

This work was partly supported by the American Diabetes Association Grant # 7–15-MI-07 (XH), NIH Grant R01 DK094025 (ZYI), and intramural institutional research funds.

Abbreviations:

Cer	ceramide
DAG	diacylglycerol
DGAT	DAG acyltransferase
FA	fatty acid or fatty acyl
LPC	lysophosphatidylcholine
LPE	lysophosphatidylethanolamine

MAG	monoacylglycerol
MDMS-SL	multi-dimensional mass spectrometry-based shotgun lipidomics
MS	mass spectrometry
NEFA	non-esterified fatty acid
PBS	phosphate buffered saline
PA	phosphatidic acid
PC	phosphatidylcholine
PE	phosphatidylethanolamine
PG	phosphatidylglycerol
PI	phosphatidylinositol
PS	phosphatidylserine
PUFA	polyunsaturated fatty acids
SM	sphingomyelin
TAG	triacylglycerol or triglyceride

References

[1]. Bays HE, “Sick fat,” metabolic disease, and atherosclerosis, Am. J. Med 122(2009) S26–S37. [PubMed: 19110085]

[2]. Flegal KM, Carroll MD, Kit BK, Ogden CL, Prevalence of obesity and trends in the distribution of body mass index among US adults, 1999–2010, JAMA 307 (2012) 491–497. [PubMed: 22253363]

[3]. Vucenik I, Stains JP, Obesity and cancer risk: evidence, mechanisms, and recommendations, Ann. N. Y. Acad. Sci 1271 (2012) 37–43. [PubMed: 23050962]

[4]. Griffin TM, Guilak F, Why is obesity associated with osteoarthritis? Insights from mouse models of obesity, Biorheology 45 (2008) 387–398. [PubMed: 18836239]

[5]. Sowers MR, Karvonen-Gutierrez CA, The evolving role of obesity in knee osteoarthritis, Curr. Opin. Rheumatol 22 (2010) 533–537. [PubMed: 20485173]

[6]. Nardone G, Ferber IA, Miller LJ, The integrity of the cholecystokinin receptor gene in gallbladder disease and obesity, Hepatology 22 (1995) 1751–1753. [PubMed: 7489984]

[7]. Grundy SM, Brewer HB, Jr., Cleeman JI, Smith SC, Jr., Lenfant C, Definition of metabolic syndrome: Report of the National heart, lung, and blood Institute/American heart Association conference on scientific issues related to definition, Circulation 109 (2004) 433–438. [PubMed: 14744958]

[8]. Wahba IM, Mak RH, Obesity and obesity-initiated metabolic syndrome: mechanistic links to chronic kidney disease, Clin. J. Am. Soc. Nephrol 2 (2007) 550–562.

[9]. Lumeng CN, Saltiel AR, Inflammatory links between obesity and metabolic disease, J. Clin. Invest 121 (2011) 2111–2117. [PubMed: 21633179]

[10]. Lau DC, Douketis JD, Morrison KM, Hramiak IM, Sharma AM, Ur E, Canadian clinical practice guidelines on the management and prevention of obesity in adults and children [summary], CMAJ 176 (2007) (2006) S1–13.

[11]. Bleich S, Cutler D, Murray C, Adams A, Why is the developed world obese?,Annu. Rev. Public Health 29 (2008) 273–295. [PubMed: 18173389]

[12]. Miller MA, Cappuccio FP, Inflammation, sleep, obesity and cardiovascular disease, Curr. Vasc. Pharmacol 5 (2007) 93–102. [PubMed: 17430213]

[13]. He Q, Wang M, Petucci C, Gardell SJ, Han X, Rotenone induces reductive stress and triacylglycerol deposition in C2C12 cells, Int. J. Biochem. Cell Biol 45 (2013) 2749–2755. [PubMed: 24104397]

[14]. Mayes JS, Watson GH, Direct effects of sex steroid hormones on adipose tissues and obesity, Obes. Rev 5 (2004) 197–216. [PubMed: 15458395]

[15]. Moellering DR, Smith DL, Jr., Ambient temperature and obesity, Curr. Obes. Rep 1 (2012) 26–34. [PubMed: 24707450]

[16]. Friedman JM, Halaas JL, Leptin and the regulation of body weight in mammals,Nature 395 (1998) 763–770. [PubMed: 9796811]

[17]. Frayn KN, Williams CM, Arner P, Are increased plasma non-esterified fatty acid concentrations a risk marker for coronary heart disease and other chronic diseases?, Clin. Sci 90 (1996) 243–253. [PubMed: 8777830]

[18]. Dole VP, A relation between non-esterified fatty acids in plasma and the metabolism of glucose, J. Clin. Invest 35 (1956) 150–154. [PubMed: 13286333]

[19]. Evans K, Burdge GC, Wootton SA, Clark ML, Frayn KN, Regulation of dietary fatty acid entrapment in subcutaneous adipose tissue and skeletal muscle, Diabetes 51 (2002) 2684–2690. [PubMed: 12196459]

[20]. Simopoulos AP, Evolutionary aspects of diet, the omega-6/omega-3 ratio and genetic variation: nutritional implications for chronic diseases, Biomed. Pharmacother 60 (2006) 502–507. [PubMed: 17045449]

[21]. Kim HK, Della-Fera M, Lin J, Baile CA, Docosahexaenoic acid inhibits adipocyte differentiation and induces apoptosis in 3T3-L1 preadipocytes, J. Nutr136 (2006) 2965–2969. [PubMed: 17116704]

[22]. Muhlhausler BS, Ailhaud GP, Omega-6 polyunsaturated fatty acids and the early origins of obesity, Curr. Opin. Endocrinol. Diabetes Obes 20 (2013) 56–61. [PubMed: 23249760]

[23]. Browning LM, n-3 Polyunsaturated fatty acids, inflammation and obesity-related disease, Proc. Nutr. Soc 62 (2003) 447–453. [PubMed: 14506893]

[24]. Cohen P, Friedman JM, Leptin and the control of metabolism: role for stearoyl-CoA desaturase-1 (SCD-1), J. Nutr 134 (2004) 2455S–2463S. [PubMed: 15333742]

[25]. Unger RH, Minireview: weapons of lean body mass destruction: the role of ectopic lipids in the metabolic syndrome, Endocrinology 144 (2003) 5159–5165. [PubMed: 12960011]

[26]. Unger RH, Lipotoxicity in the pathogenesis of obesity-dependent NIDDM. genetic and clinical implications, Diabetes 44 (1995) 863–870. [PubMed: 7621989]

[27]. Day C, Bailey CJ, Obesity in the pathogenesis of type 2 diabetes, Br. J. Diabetes Vasc. Dis 11 (2011) 55–61.

[28]. Garris DR, Cytochemical analysis of pancreatic islet lipoapoptosis: hyperlipidemia-induced cytoinvolution following expression of the diabetes (db/ db) mutation, Pathobiology 72 (2005) 124–132. [PubMed: 15860929]

[29]. Shimabukuro M, Zhou YT, Levi M, Unger RH, Fatty acid-induced beta cell apoptosis: a link between obesity and diabetes, Proc. Natl. Acad. Sci. USA 95 (1998) 2498–2502. [PubMed: 9482914]

[30]. Summers SA, Ceramides in insulin resistance and lipotoxicity, Prog. Lipid Res. 45 (2006) 42–72. [PubMed: 16445986]

[31]. Wei Y, Wang D, Topczewski F, Pagliassotti MJ, Saturated fatty acids induce endoplasmic reticulum stress and apoptosis independently of ceramide in liver cells, Am. J. Physiol. Endocrinol. Metab 291 (2006) E275–E281. [PubMed: 16492686]

[32]. Turpin SM, Ryall JG, Southgate R, Darby I, Hevener AL, Febbraio MA, Kemp BE, Lynch GS, Watt MJ, Examination of ‘lipotoxicity’ in skeletal muscle of high-fat fed and ob/ ob mice, J. Physiol 587 (2009) 1593–1605. [PubMed: 19204053]

[33]. Sparagna GC, Hickson-Bick DL, Buja LM, McMillin JB, A metabolic role for mitochondria in palmitate-induced cardiac myocyte apoptosis, Am. J. Physiol. Heart Circ. Physiol 279 (2000) H2124–H2132. [PubMed: 11045945]

[34]. Han X, Gross RW, Shotgun lipidomics: electrospray ionization mass spectro-metric analysis and quantitation of the cellular lipidomes directly from crude extracts of biological samples, Mass Spectrom. Rev 24 (2005) 367–412. [PubMed: 15389848]

[35]. Han X, Yang K, Gross RW, Multi-dimensional mass spectrometry-based shotgun lipidomics and novel strategies for lipidomic analyses, Mass Spectrom, Rev 31 (2012) 134–178. [PubMed: 21755525]

[36]. Yang K, Cheng H, Gross RW, Han X, Automated lipid identification and quantification by multi-dimensional mass spectrometry-based shotgun lipidomics, Anal. Chem 81 (2009) 4356–4368. [PubMed: 19408941]

[37]. Wang M, Han X, Multidimensional mass spectrometry-based shotgun lipidomics, Methods Mol. Biol 1198 (2014) 203–220. [PubMed: 25270931]

[38]. Han X, Lipidomics: comprehensive mass spectrometry of lipids, John Wiley & Sons, Inc., Hoboken, New Jersey, 2016.

[39]. Wang M, Hayakawa J, Yang K, Han X, Characterization and quantification of diacylglycerol species in biological extracts after one-step derivatization: a shotgun lipidomics approach, Anal. Chem 86 (2014) 2146–2155. [PubMed: 24432906]

[40]. Wang M, Han RH, Han X, Fatty acidomics: Global analysis of lipid species containing a carboxyl group with a charge-remote fragmentation-assisted approach, Anal. Chem 85 (2013) 9312–9320. [PubMed: 23971716]

[41]. Wang M, Wang C, Han RH, Han X, Novel advances in shotgun lipidomics for biology and medicine, Prog. Lipid Res 61 (2016) 83–108. [PubMed: 26703190]

[42]. Han X, Yang K, Gross RW, Microfluidics-based electrospray ionization enhances intrasource separation of lipid classes and extends identification of individual molecular species through multi-dimensional mass spectrometry: development of an automated high throughput platform for shotgun lipidomics, Rapid Commun. Mass Spectrom 22 (2008) 2115–2124. [PubMed: 18523984]

[43]. Wang C, Wang M, Han X, Comprehensive and quantitative analysis of lysophospholipid molecular species present in obese mouse liver by shotgun lipidomics, Anal. Chem 87 (2015) 4879–4887. [PubMed: 25860968]

[44]. Yang K, Han X, Accurate quantification of lipid species by electrospray ionization mass spectrometry - Meets a key challenge in lipidomics, Metabolites 1 (2011) 21–40. [PubMed: 22905337]

[45]. Wang M, Wang C, Han X, Selection of internal standards for accurate quanti-fication of complex lipid species in biological extracts by electrospray ionization mass spectrometry-What, how and why?, Mass Spectrom. Rev (2016). 10.1002/mas.21492.

[46]. Han RH, Wang M, Fang X, Han X, Simulation of triacylglycerol ion profiles: bioinformatics for interpretation of triacylglycerol biosynthesis, J. Lipid Res. 54 (2013) 1023–1032. [PubMed: 23365150]

[47]. Han X, Gross RW, Quantitative analysis and molecular species fingerprinting of triacylglyceride molecular species directly from lipid extracts of biological samples by electrospray ionization tandem mass spectrometry, Anal. Biochem 295 (2001) 88–100. [PubMed: 11476549]

[48]. Garbarino J, Sturley SL, Saturated with fat: new perspectives on lipotoxicity, Curr. Opin. Clin. Nutr. Metab. Care 12 (2009) 110–116. [PubMed: 19202381]

[49]. Athenstaedt K, Daum G, The life cycle of neutral lipids: synthesis, storage and degradation, Cell. Mol. Life Sci. 63 (2006) 1355–1369. [PubMed: 16649142]

[50]. Guillou H, Zadravec D, Martin PG, Jacobsson A, The key roles of elongases and desaturases in mammalian fatty acid metabolism: insights from transgenic mice, Prog. Lipid Res 49 (2010) 186–199. [PubMed: 20018209]

[51]. Kaur N, Chugh V, Gupta AK, Essential fatty acids as functional components of foods- a review, J. Food Sci. Technol 51 (2014) 2289–2303. [PubMed: 25328170]

[52]. Breuer B, Stuhlfauth T, Fock H, Huber H, Fatty acids of some cornaceae, hydrangeaceae, aquifoliaceae, hamamelidaceae and styracaceae, Phytochemistry 26 (1987) 1441–1445.

[53]. Rudkowska I, Roynette CE, Demonty I, Vanstone CA, Jew S, Jones PJ, Diacylglycerol: efficacy and mechanism of action of an anti-obesity agent, Obes. Res 13 (2005) 1864–1876. [PubMed: 16339116]

[54]. Han MS, Park SY, Shinzawa K, Kim S, Chung KW, Lee JH, Kwon CH, Lee KW, Park CK, Chung WJ, Hwang JS, Yan JJ, Song DK, Tsujimoto Y, Lee MS, Lysophosphatidylcholine as a death effector in the lipoapoptosis of hepatocytes, J. Lipid Res 49 (2008) 84–97. [PubMed: 17951222]

[55]. Erion DM, Shulman GI, Diacylglycerol-mediated insulin resistance, Nat. Med 16 (2010) 400–402. [PubMed: 20376053]

[56]. Czabany T, Athenstaedt K, Daum G, Synthesis, storage and degradation of neutral lipids in yeast, Biochim. Biophys. Acta 1771 (2007) 299–309. [PubMed: 16916618]

[57]. Walther TC, Farese RV, Jr., The life of lipid droplets, Biochim. Biophys. Acta 1791 (2009) 459–466. [PubMed: 19041421]

[58]. Chavez JA, Summers SA, Characterizing the effects of saturated fatty acids on insulin signaling and ceramide and diacylglycerol accumulation in 3T3-L1 adipocytes and C2C12 myotubes, Arch. Biochem. Biophys 419 (2003) 101–109. [PubMed: 14592453]

[59]. Muzzin P, Eisensmith RC, Copeland KC, Woo SL, Correction of obesity and diabetes in genetically obese mice by leptin gene therapy, Proc. Natl. Acad. Sci. USA 93 (1996) 14804–14808. [PubMed: 8962136]

[60]. Bray GA, York DA, Hypothalamic and genetic obesity in experimental animals: an autonomic and endocrine hypothesis, Physiol. Rev 59 (1979) 719–809. [PubMed: 379887]

[61]. Yoshihara E, Fujimoto S, Inagaki N, Okawa K, Masaki S, Yodoi J, Masutani H, Disruption of TBP-2 ameliorates insulin sensitivity and secretion without affecting obesity, Nat. Commun 1 (2010) 127. [PubMed: 21119640]

[62]. Cusi K, Role of obesity and lipotoxicity in the development of nonalcoholic steatohepatitis: pathophysiology and clinical implications, Gastroenterology 142 (2012) 711 e716–725 e716. [PubMed: 22326434]

[63]. Bugianesi E, Gastaldelli A, Vanni E, Gambino R, Cassader M, Baldi S, Ponti V, Pagano G, Ferrannini E, Rizzetto M, Insulin resistance in non-diabetic patients with non-alcoholic fatty liver disease: sites and mechanisms, Diabetologia 48 (2005) 634–642. [PubMed: 15747110]

[64]. Guo ZK, Intramyocellular lipid kinetics and insulin resistance, Lipids Health Dis. 6 (2007) 18. [PubMed: 17650308]

[65]. Holland WL, Brozinick JT, Wang LP, Hawkins ED, Sargent KM, Liu Y, Narra K, Hoehn KL, Knotts TA, Siesky A, Nelson DH, Karathanasis SK, Fontenot GK, Birnbaum MJ, Summers SA, Inhibition of ceramide synthesis ameliorates glucocorticoid-, saturated-fat-, and obesity-induced insulin resistance, Cell Metab. 5 (2007) 167–179. [PubMed: 17339025]

[66]. Watson ML, Coghlan M, Hundal HS, Modulating serine palmitoyl transferase (SPT) expression and activity unveils a crucial role in lipid-induced insulin resistance in rat skeletal muscle cells, Biochem. J 417 (2009) 791–801. [PubMed: 18922131]

[67]. Olefsky JM, Glass CK, Macrophages, inflammation, and insulin resistance, Annu. Rev. Physiol 72 (2010) 219–246. [PubMed: 20148674]

[68]. Marfella R, Di Filippo C, Portoghese M, Barbieri M, Ferraraccio F, Siniscalchi M, Cacciapuoti F, Rossi F, D'Amico M, Paolisso G, Myocardial lipid accumulation in patients with pressure-overloaded heart and metabolic syndrome, J. Lipid Res. 50 (2009) 2314–2323. [PubMed: 19470430]

[69]. Kawai K, Sakairi T, Harada S, Shinozuka J, Ide M, Sato H, Tanaka M, Toriumi W, Kume E, Diet modification and its influence on metabolic and related pathological alterations in the SHR/NDmcr-cp rat, an animal model of the metabolic syndrome, Exp. Toxicol. Pathol 64 (2012) 333–338. [PubMed: 20965707]

[70]. Karahashi M, Ishii F, Yamazaki T, Imai K, Mitsumoto A, Kawashima Y, Kudo N, Up-regulation of stearoyl-CoA desaturase 1 increases liver MUFA content in obese Zucker but not Goto-Kakizaki rats, Lipids 48 (2013) 457–467. [PubMed: 23539346]

[71]. Aguilar PS, de Mendoza D, Control of fatty acid desaturation: a mechanism conserved from bacteria to humans, Mol. Microbiol 62 (2006) 1507–1514. [PubMed: 17087771]

[72]. Liang CP, Tall AR, Transcriptional profiling reveals global defects in energy metabolism, lipoprotein, and bile acid synthesis and transport with reversal by leptin treatment in ob/ ob mouse liver, J. Biol. Chem 276 (2001) 49066–49076. [PubMed: 11551957]

[73]. Ferrante AW, Jr., M. Thearle, T. Liao, R.L. Leibel, Effects of leptin deficiency and short-term repletion on hepatic gene expression in genetically obese mice, Diabetes 50 (2001) 2268–2278. [PubMed: 11574408]

[74]. Ntambi JM, Miyazaki M, Stoehr JP, Lan H, Kendziorski CM, Yandell BS, Song Y, Cohen P, Friedman JM, Attie AD, Loss of stearoyl-CoA desaturase-1 function protects mice against adiposity, Proc. Natl. Acad. Sci. USA 99 (2002) 11482–11486. [PubMed: 12177411]

[75]. Herberg L, Coleman DL, Laboratory animals exhibiting obesity and diabetes syndromes, Metabolism 26 (1977) 59–99. [PubMed: 834144]

[76]. Tripathy S, Jump DB, Elovl5 regulates the mTORC2-Akt-FOXO1 pathway by controlling hepatic cis-vaccenic acid synthesis in diet-induced obese mice, J. Lipid Res 54 (2013) 71–84. [PubMed: 23099444]

[77]. Riccardi G, Giacco R, Rivellese AA, Dietary fat, insulin sensitivity and the metabolic syndrome, Clin. Nutr 23 (2004) 447–456. [PubMed: 15297079]

[78]. Cheng H, Guan S, Han X, Abundance of triacylglycerols in ganglia and their depletion in diabetic mice: implications for the role of altered triacylglycerols in diabetic neuropathy, J. Neurochem 97 (2006) 1288–1300. [PubMed: 16539649]

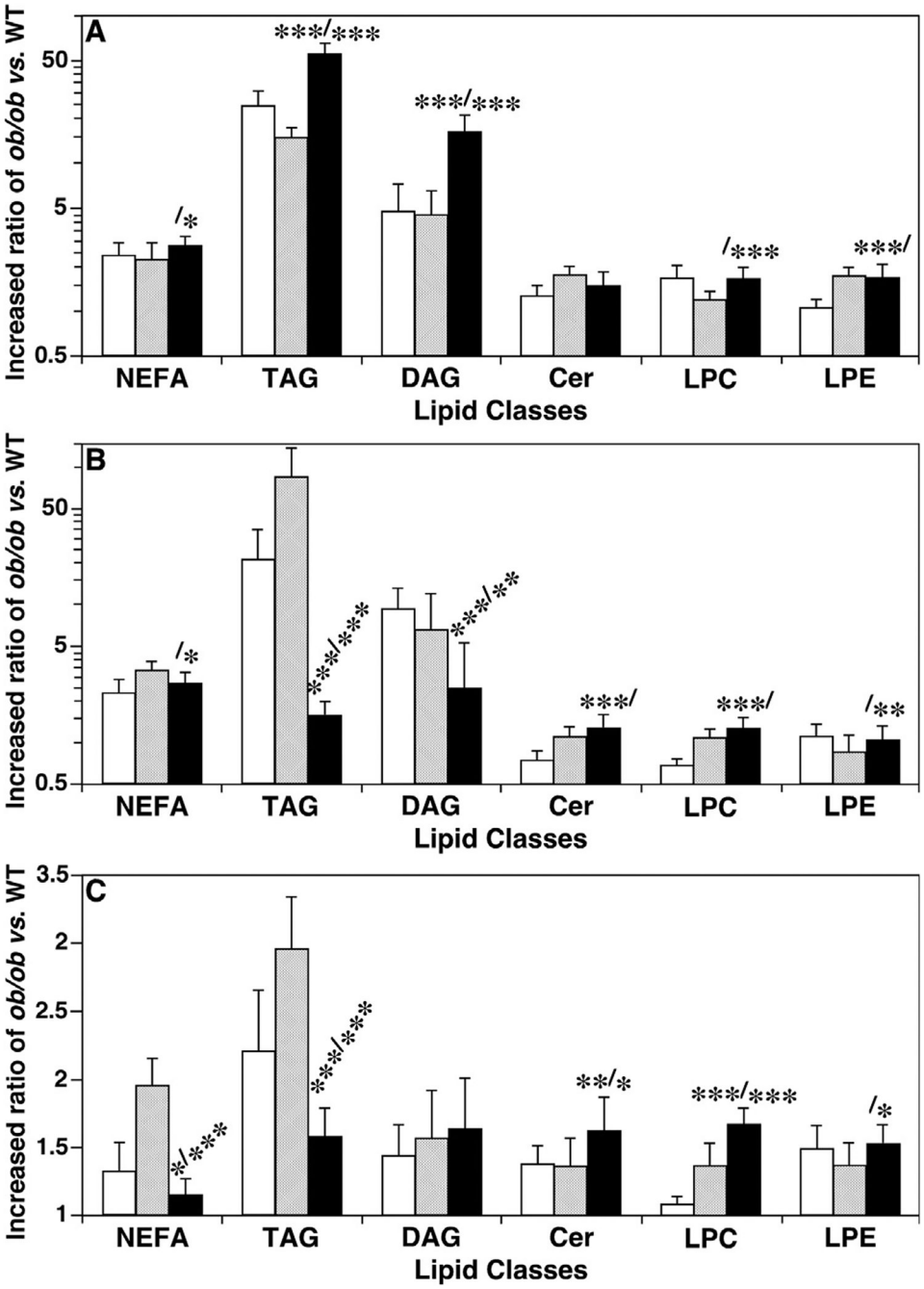

Fig. 1.

Temporal comparison of the increased ratios of lipotoxic lipid levels in the liver, muscle and heart of ob/ ob mice vs. their controls. Ratios were calculated by the lipid mass levels (accumulation of which represents lipotoxicity, and could lead to cell dysfunction or cell death) in ob/ ob vs WT mouse liver (Panel A), thigh skeletal muscle (Panel B), and heart (Panel C) at 10 (open bars), 12 (shaded bars), and 16 weeks (solid bars) of age by MDMS-SL as described in MATERIALS AND METHODS. NEFA, TAG, DAG, Cer, LPC, and LPE stand for non-esterified fatty acid, triacylglycerol, diacylglycerol, ceramide,

lysophosphatidylcholine, and lysophosphatidylethanolamine, respectively. The statistical symbols indicate the statistical differences between 10 and 16 weeks (the symbols before the slash) and between 12 and 16 weeks (the symbols after the slash).

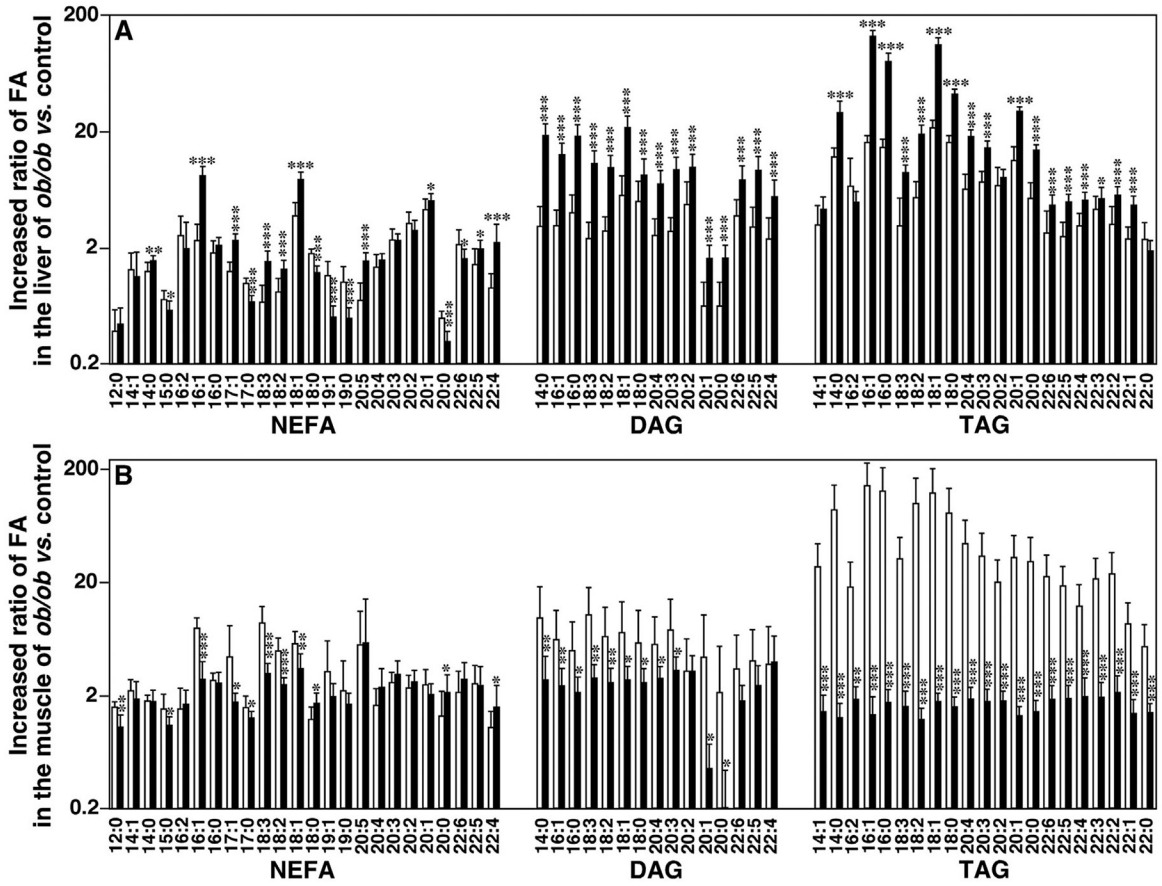

Fig. 2.

Temporal comparison of ratios of fatty acyl chains in liver and thigh skeletal muscle of ob/ob mice vs. controls. Ratios were calculated by mass levels of non-esterified fatty acid (NEFA), diacylglycerol (DAG), and triacylglycerol (TAG) in mouse liver (Panel A) and thigh skeletal muscle (Panel B) at 12 (open bars) and 16 weeks (solid bars) of age by MDMS-SL as described in MATERIALS AND METHODS. Fatty acyl (FA) chain content in DAG and TAG was calculated from mass levels of individual species. Statistical significance was determined by a two-tailed Student t-test in comparisons with control, in which *$p < 0.05$, **$p < 0.01$, and ***$p < 0.001$.

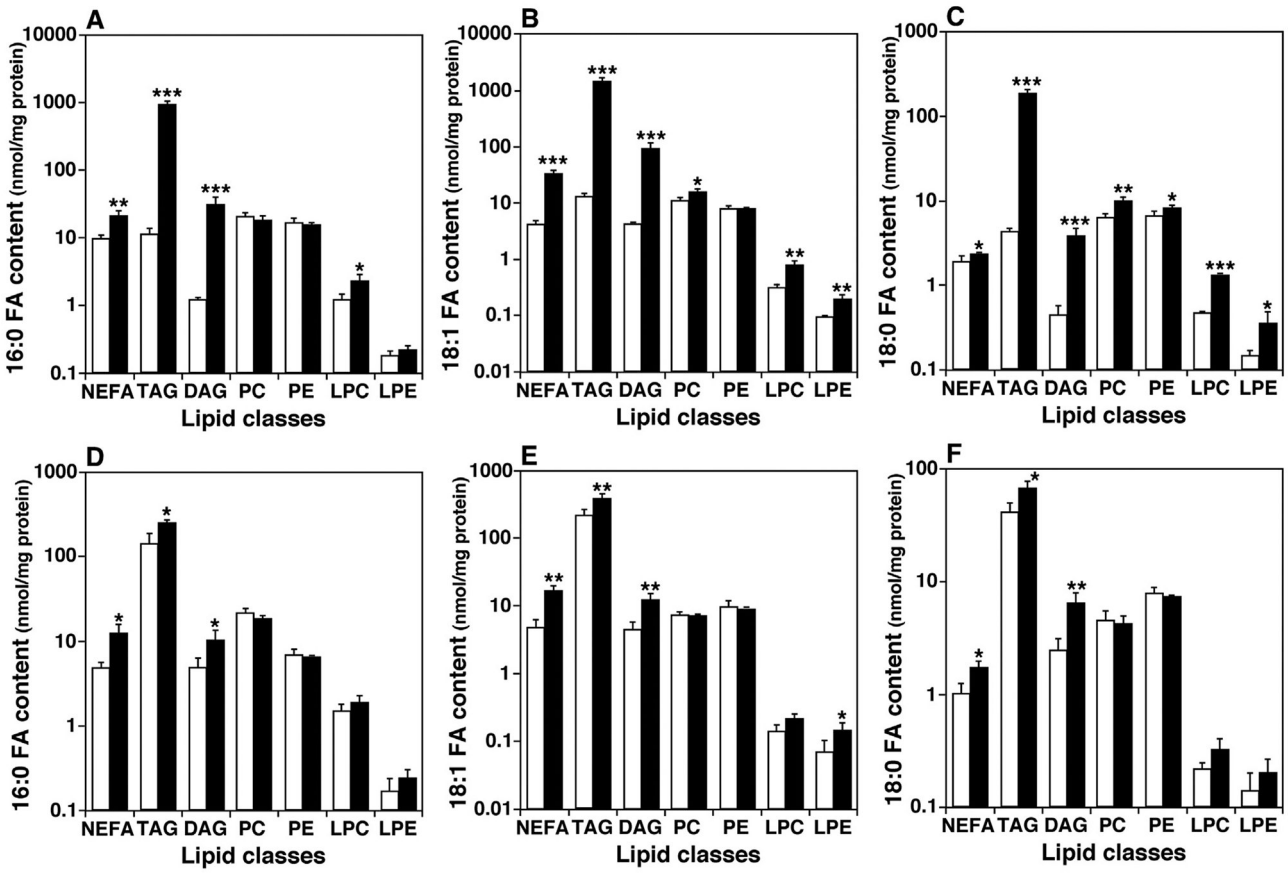

Fig. 3.

Comparison of the mass levels of fatty acyl chains (16:0, 18:0 and 18:1) in different lipid classes in the liver and skeletal muscle between ob/ ob mice and their controls. The mass levels of lipids were determined in mouse liver (Panels A to C) and thigh skeletal muscle (Panels D to F) of ob/ ob mice (solid bars) and their controls (open bars) at 16 weeks of age by MDMS-SL as described in MATERIALS AND METHODS. The content of 16:0 (Panels A and D), 18:1 (Panels B and E), and 18:0 (Panels C and F) fatty acyl (FA) chains in the indicated lipid classes (except non-esterified fatty acid (NEFA)) were calculated from the mass levels of individual species of the corresponding lipid classes. TAG, DAG, PC, PE, LPC, and LPE stand for triacylglycerol, diacylglycerol, phosphatidylcholine, phosphatidylethanolamine, lysophosphatidylcholine, and lysophosphatidylethanolamine, respectively.

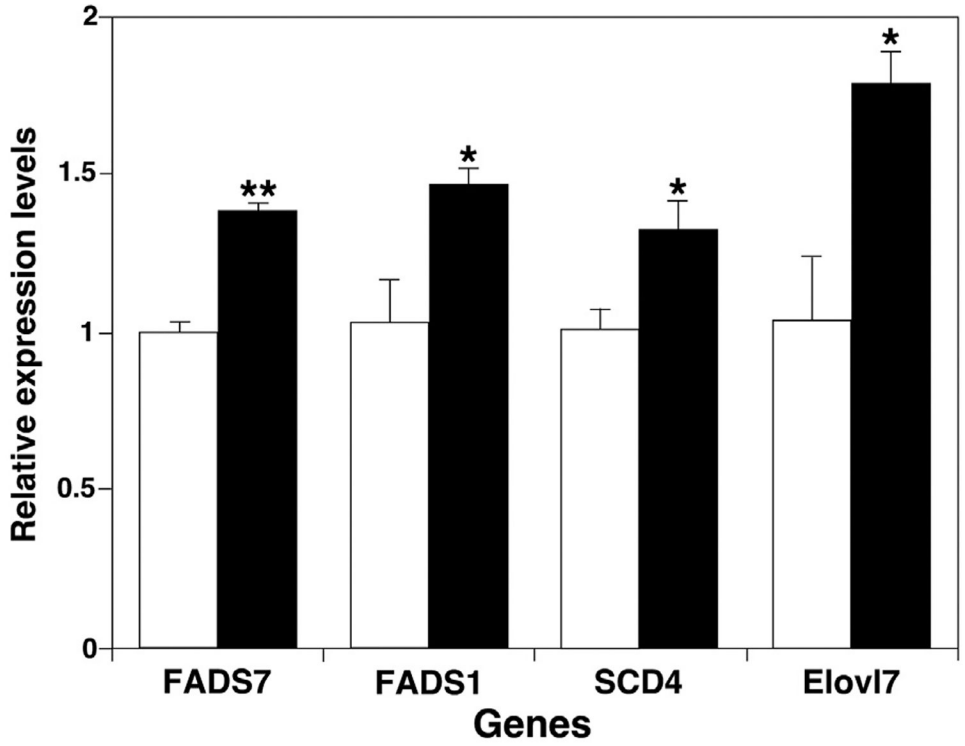

Fig. 4.

Comparison between ob/ ob mice and their controls of expression levels of genes involved in de novo fatty acid synthesis in skeletal muscle. Expression of fatty acid desaturase (FADS), fatty acid elongase (Elovl), and stearoyl-CoA desaturase (SCD) genes in thigh skeletal muscle of ob/ ob mice (Solid bars) and their controls (open bars) at 16 weeks of age was measured by real-time RT-PCR as described in MATERIALS AND METHODS. Data are presented after normalization to cyclophilin expression.

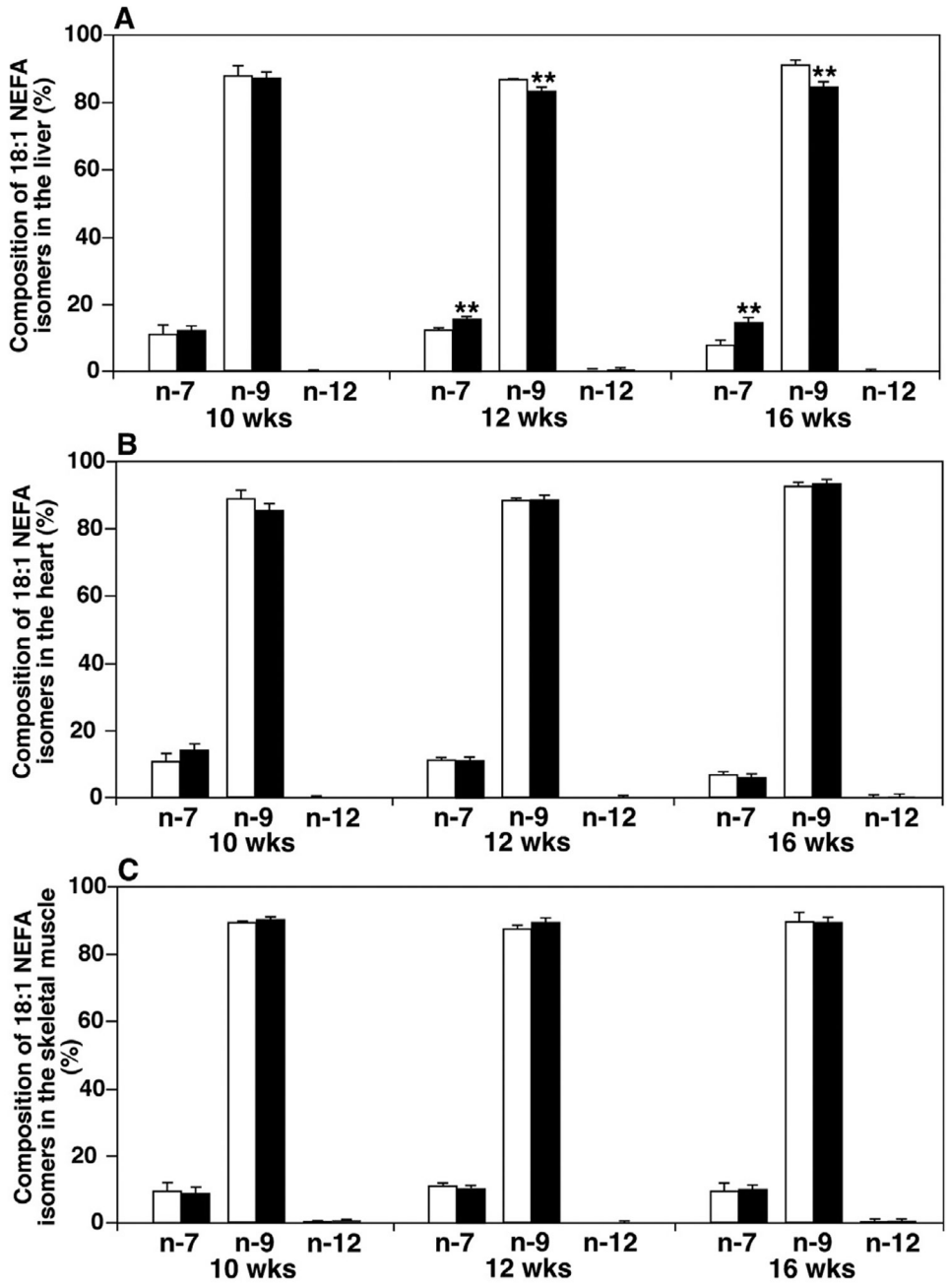

Fig. 5.

Temporal comparison of 18:1 fatty acid isomers in liver, heart, and skeletal muscle of ob/ ob mice to their controls. The composition of non-esterified 18:1 fatty acid (18:1 NEFA) isomers was determined in mouse liver (Panel A), heart (Panel B), and thigh skeletal muscle (Panel C) of ob/ ob mice (solid bars) and their controls (open bars) at 10, 12, and 16 weeks of age by MDMS-SL as described in MATERIALS AND METHODS. These isomers include vaccenic (n-7), oleic (n-9), and petroselinic (n-12) acids as indicated.

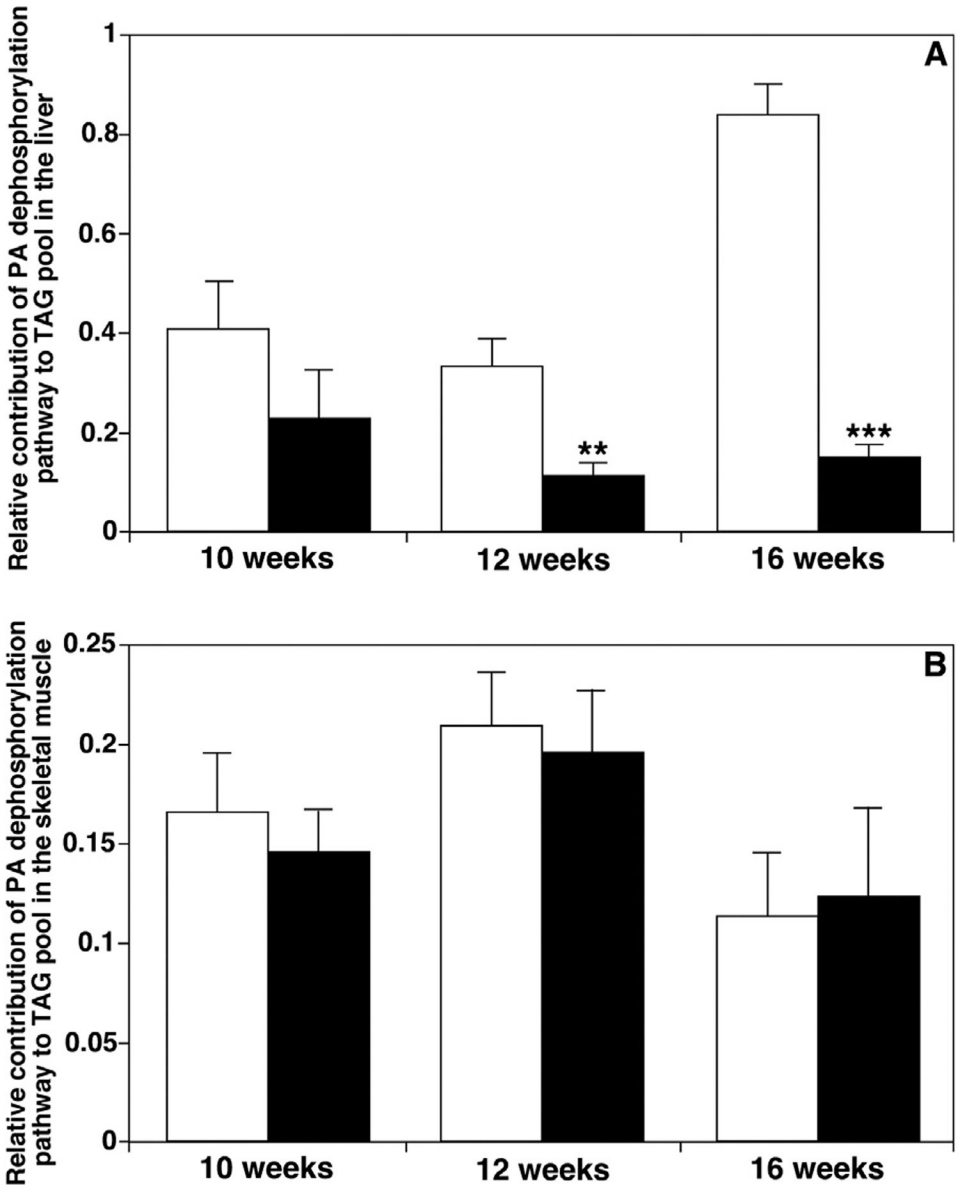

Fig. 6.

Temporal comparison of the relative contributions of different triacylglycerol biosynthesis pathways to fat pools in liver and muscle between ob/ ob mice vs. their controls. Comprehensive cellular lipidomes of mouse organs were determined by MDMSSL as described in MATERIALS AND METHODS. The contributions of different triacylglycerol (TAG) biosynthesis pathways to TAG pools in mouse liver (Panel A) and thigh skeletal muscle (Panel B) of ob/ ob mice (solid bars) and their controls (open bars) at 10, 12, and 16 weeks of age were simulated using lipidomics data as previously described in detail [46]. These pathways represent the diacylglycerol generation, including phosphatidic acid dephosphorylation (K1), monoacylglycerol reacylation (K2), and hydrolysis of phospholipid head groups (K3). It was found that the pathway K3 was negligible in the current study. Thus, K1+ K2=1.

Table 1

Amounts of lipids accumulated in the liver, heart, kidney, and skeletal muscle of ob/ ob mice in comparison to their WT controls at 12 weeks of age.

Lipid	Liver			Heart			Kidney			Skeletal muscle		
class	WT	ob/ ob	T-test	WT	ob/ ob	T-test	WT	ob/ ob	T-test	WT	ob/ ob	T-test
LPE	0.71 ± 0.04	1.22 ± 0.17		0.74 ± 0.07	1.02 ± 0.09	**	1.31 ± 0.17	1.19 ± 0.18		0.23 ± 0.06	0.19 ± 0.06	
LPC	6.18 ± 0.55	7.48 ± 0.56	*	2.63 ± 0.30	3.60 ± 0.11	**	4.48 ± 0.12	4.31 ± 0.04		1.74 ± 0.16	1.91 ± 0.22	
Cer	0.89 ± 0.09	1.56 ± 0.15	**	0.36 ± 0.03	0.49 ± 0.06	*	1.69 ± 0.14	1.65 ± 0.08		0.59 ± 0.09	0.65 ± 0.05	
TAG	62.13 ± 1.36	947.02 ± 129.97	***	15.04 ± 1.61	44.51 ± 3.24	***	13.79 ± 2.59	20.33 ± 4.25		16.27 ± 1.92	1391.22 ± 853.71	*
DAG	16.47 ± 4.36	75.31 ± 24.44	*	4.01 ± 0.70	6.30 ± 0.86	**	4.70 ± 0.36	5.42 ± 0.76		4.31 ± 0.81	28.49 ± 22.9	
NEFA	48.56 ± 10.52	110.47 ± 15.46	**	54.56 ± 5.13	106.84 ± 4.78	***	15.67 ± 0.23	19.9 ± 0.61	**	5.23 ± 0.31	17.47 ± 2.63	**

The data represent mean ± SD in nmol/ mg. Statistical significance was determined by a two-tailed student t-test in comparison to control, where *, **, and *** indicate $p < 0.05$, 0.01, and 0.001, respectively.